Fine structure in the energy dependence of current density and oscillations in the current-voltage characteristics of tunnel junctions

Anatoly Grinberg and Serge Luryi

AT&T Bell Laboratories, Murray Hill, New Jersey 07974

(Received 11 December 1989)

We present a theoretical model for the current oscillations observed in tunnel heterojunction diodes. The model is based on the assumption that the only scattering mechanisms operating in the active region of the diode are due to the electron interaction with optical phonons and charged impurities. This allows us to introduce a new transport characteristic, the reduced differential current, whose divergence vanishes. This property (similar to that of the total current) gives a constructive way of determining the mobility in a quasineutral region of the sample, whose modulation by the applied voltage leads to the observed current oscillations. We argue that the current in the quasineutral region is space-charge-limited and can be calculated within the virtual-cathode approximation. Existence of a virtual cathode is due to a large thermodiffusive component of the current at the boundary between the depletion and quasineutral regions, where electrons lose most of their kinetic energy over a short distance. The calculated current oscillations are in good quantitative agreement with experiment.

I. INTRODUCTION

Current-voltage characteristics of single-barrier n^+GaAs/(Al,Ga)As/n^-GaAs/n^+GaAs heterostructures (current direction perpendicular to the barrier) show an oscillatory structure with a characteristic period $e\Delta V=\hbar\omega$ in applied voltage V corresponding to the energy $\hbar\omega=36$ meV of the LO phonon in GaAs. This effect was originally discovered by Hickmott et al.[1] in an external magnetic field $B \gtrsim 4$ T; subsequently, Eaves et al.[2] have observed a similar structure at $B=0$. Experimentally, the oscillations in current J itself are weak, $\Delta J/J \sim 10^{-3}$, but in derivative plots, dJ/dV and, especially, d^2J/dV^2 versus V, they are seen very clearly. Energy-band diagram of a typical experimental sample is illustrated in Fig. 1. For a detailed discussion of recent experimental work the reader is referred to Ref. 9.

A number of theoretical models have been proposed to explain this phenomenon.[3-8] Most of the proposed models agree that interaction with optical phonons during the tunneling process itself is not important. To a good approximation, the tunneling probability depends only on the voltage drop across the (AlGa)As barrier and is not affected by phonons. Interaction with optical phonons can tangibly influence only the resistance of the lightly doped n^-GaAs layer that in turn affects the voltage drop across the barrier and hence the current. The difference between various models mainly consists in the specific mechanism of the resistance modulation—based on different assumptions about the formation of current in the n^-GaAs region of the device.

Several authors[1,4,7] assumed that due to a freeze-out of electrons there is no depletion region in the low-doped part of the diode. This assumption is untenable.[9] In a strong electric field of the typical experiment, the freeze-out state (unstable against various perturbations, such as impact ionization, hopping conduction, field ionization, etc.) will go over into a stable configuration with the depletion region formed. It is unlikely that the unstable state could persist for the duration of an experiment.

Eaves et al.[3] based their consideration on a more realistic model of the field distribution in the n^-GaAs layer—with a usual separation of that layer into a depleted and a quasineutral (QN) region. It has been assumed that electrons emit all possible LO phonons in the depleted region and that no other inelastic processes occur within that region. Consequently, electrons entering the QN region have a kinetic energy within the interval $(0,\hbar\omega)$. If the initial energy distribution of electrons tunneling through an (AlGa)As barrier is sharply peaked, then this peak is somewhat replicated within the interval $(0,\hbar\omega)$ in the QN region. The key idea of Eaves et al.[3] is that these hot electrons entering the QN region modulate its conductivity by impact ionizing the donor centers and that effectiveness of this process depends on the position of the energy distribution peak. If the peak is below donor ionization threshold, then impact ionization is suppressed. Position of the peak is assumed to be periodically modulated as the voltage is applied to the device, wherein, according to the model, lies the origin of the current oscillations.

The model of Eaves et al.[3] assumes a coexistence in the QN region of two groups of carriers: hot electrons entering from the depletion layer and secondary electrons produced by impact ionization of shallow donors in the QN layer.[10] The model does not offer a constructive way of estimating either the relative concentration of these two groups or the total concentration of mobile carriers in the QN region.[11] Moreover, there is a fundamental reason for doubting the validity of this model. Its main assumption consists in postulating that in the QN region the electron energy distribution is periodically modulated

by V. Presumably, this property arises from a replication of the initial electron energy distribution at the tunneling barrier. Given that optical-phonon scattering is the only inelastic interaction, this assumption appears plausible and, for a very narrow, "δ function," initial distributions, it is undoubtedly correct. However, as will be shown
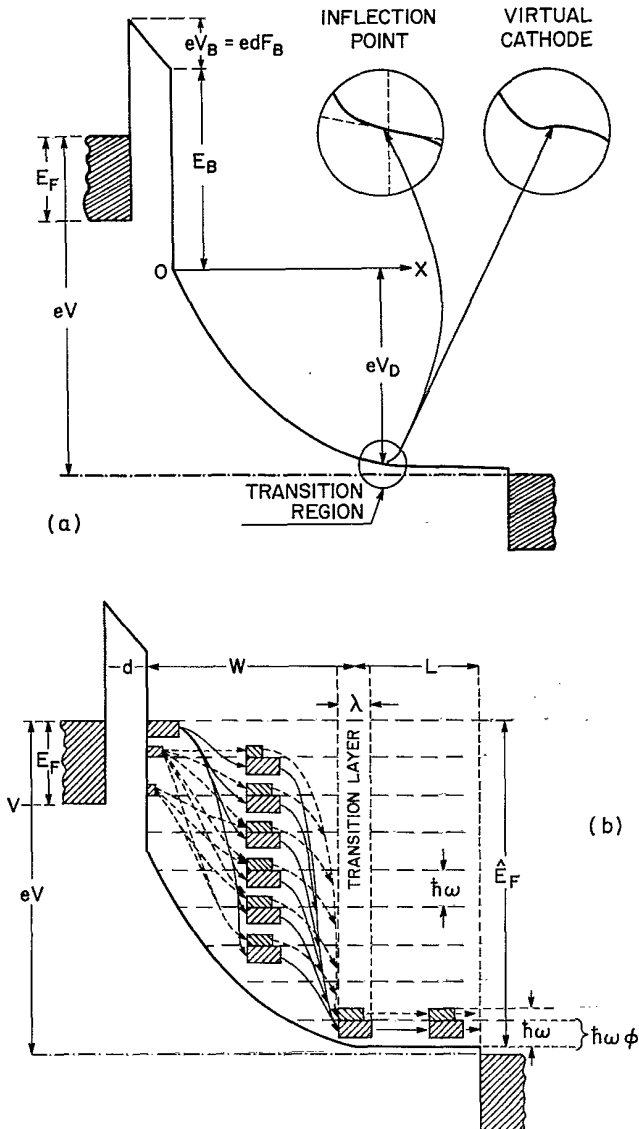

FIG. 1. (a) Schematic energy-band diagram of a sample under bias. Insets illustrate the formation of the virtual cathode in the transition regime between the depletion layer and the QN layer. Left inset shows a hypothetical band diagram in the absence of hot-electron effects. Inflection point of the electrostatic potential and the field at that point are shown by dashed lines. Right inset shows the band diagram in the presence of thermodiffusion in the transition layer. (b) Redistribution of differential currents through the device. Evolution of currents originating in three different energy intervals is traced. Dashed lines trace the currents which can mix in the process of transport. In passing through the low-field transition layer, all elementary currents concentrate in a reduced energy interval within $\hbar\omega$ from the conduction-band edge. Also shown is the phase Φ defined by Eq. (6).

below (in connection with Fig. 2), the energy distribution of electrons injected by tunneling from a degenerately doped emitter is not narrow on the scale of $\hbar\omega$. Any initial distribution of finite width is distorted in transport through the depletion region. This distortion is brought about by the difference in the drift of electrons belonging to different energy intervals. It, moreover, depends on the total voltage drop in the depletion region, i.e., also on V. Whether or not there is even an *approximate* periodicity in the electron energy distribution in the QN layer depends on the form of the initial distribution and requires further assumptions about the elastic scattering rate $\tau(E)$. This question can hardly be ascertained without tracing the electron transport in detail.

What is rigorously conserved in any scattering model that takes LO-phonon scattering to be the only inelastic interaction, is the *reduced differential current* (RDC). The RDC is defined (Sec. II) as the sum of the differential currents $dJ(E)/dE$, over a discrete set of energies E differing by an integral number of optical-phonon energies $\hbar\omega$. Here E is the total electron energy, including both the kinetic energy and the potential energy $E_C(x)$.

This notion of a spatially invariant periodic RDC function is the key ingredient of our model. Because of the energy dependence of the elastic scattering rate governing the mobility μ, the nearly periodic variation of the RDC with the applied voltage translates into a modulation of μ in the QN region. The current in that region is shown to be of space-charge-limited nature. The periodic variation in μ causes a similar variation in the voltage drop in the QN layer; despite its smallness, this variation affects the voltages in other regions of the diode, resulting in a modulation of the tunnel current. Detailed qualitative description of our model is presented in Sec. II. In Sec. III, we derive the complete current-voltage characteristics of the diode.

II. QUALITATIVE DESCRIPTION OF THE MODEL

Let us first compare the characteristic electron scattering rates with the transit time through the active regions of the device. Estimates show that at electron kinetic energies of order $\hbar\omega$, the energy relaxation time due to emission of acoustic phonons is of order 10^{-10} s. This is much longer than the electron transit time through the entire lightly doped layer. Indeed, the slowest transport occurs in the QN region, where the dominant scattering mechanism is interaction with ionized impurities. At the impurity concentrations of order 10^{15} cm^{-3}, the mobility, calculated for this process, is $\mu \gtrsim 10^5$ cm^2/V s. As we shall see in Sec. III, the range of interest in IV characteristics corresponds to typical electric fields $F \gtrsim 10$ V/cm in the QN region. This implies a drift velocity $v_d \gtrsim 10^6$ cm/s and a transit time less than 10^{-8} s. Consequently, the energy relaxation on acoustic phonons in the active region of the device is entirely negligible. Because of the low carrier concentration in the lightly doped layer, electron-electron scattering can be safely neglected also. This leaves optical-phonon scattering as the only inelastic process. Under such conditions, electronic

transport exhibits unusual features, the most striking of which is the appearance of a new transport invariant, the reduced differential current.

A. Conservation of the reduced differential current

Consider a group of electrons tunneling into the semiconductor in a small interval ΔE at an energy E measured from a fixed level. These electrons carry a current

$$(\Delta J(E))_B = \left[\frac{\partial J}{\partial E}\right]_B \Delta E \ , \tag{1}$$

where the subscript B denotes quantities evaluated at the barrier interface $x = 0$. In the process of acceleration by the electric field, this group of electrons spreads over discrete levels

$$E_\nu(E) = E + \nu \hbar \omega, \quad \nu = 0, \pm 1, \pm 2, \ldots, \quad E_\nu \geq E_C(x) \ , \tag{2}$$

which differ from E by an integral number of LO-phonon energies. It may appear that the sum of the currents carried by electrons in all these discrete levels equals $\Delta J(E)|_B$. However, if the initial energy distribution of the tunneling current was wider than $\hbar \omega$, then currents originating from initial energy intervals, different by an integral number of optical-phonon energies, may mix together in the process of drift [see Fig. 1(b)]. Let us, therefore, extend the initial group to include all electrons in the initial distribution at energies differing by $\hbar \omega$. In the process of transport, this extended group will also spread over the levels $E_\nu(E)$. Denote by $n_{\text{ext}}(E)$ the total carrier concentration in the extended group and by $G(E,x)$ the total current carried by electrons in this group. The extended group is a closed system in our scattering model and, therefore, it must obey the current-continuity condition

$$\frac{e \partial n_{\text{ext}}(E)}{\partial t} + \nabla \cdot \mathbf{G}(E) = 0 \ , \tag{3}$$

where

$$\mathbf{G}(E) = \sum_\nu \left.\frac{\partial \mathbf{J}}{\partial E}\right|_{E + \nu \hbar \omega} \ , \quad \nu = 0, \pm 1, \pm 2, \ldots \ . \tag{4}$$

Equation (4) defines the RDC function. In a steady state, $G(E)$ is a conserved quantity.

B. Energy distribution of the current in the quasineutral region

From the definition of the RDC, Eq. (4), it is clear that it is a periodic function of energy with the period $\hbar \omega$. Even though $G(E)$ is conserved, we cannot extract from it the energy distribution of the current in an arbitrary cross section of the sample. However, if, for some reason, the kinetic energy of all electrons in a given cross section does not exceed $\hbar \omega$, then we have

$$\frac{\partial J}{\partial E} = G(E) \ . \tag{5}$$

This condition would be naturally satisfied at any point, if

the rate LO-phonon emission were very high, i.e., in the limit $\tau_{\text{opt}} \rightarrow 0$. In that hypothetical limit, electrons do not acquire energies over $\hbar \omega$. It should be clearly understood that our model assumes no such "coherence" in phonon emission. The coherence issue was recently investigated[8] by a Monte Carlo simulation of electron transport in the depletion region of a lightly doped GaAs diode. It was found that the average electron energy at the end of that region was substantially *higher* than $\hbar \omega$. This shows only that τ_{opt} is insufficiently short, i.e., that the mean free path $\lambda_{\text{opt}} > \hbar \omega / eF$ and electrons are still spread over the levels E_ν [Eq. (2)]. It would be more interesting to study numerically the energy distributions of currents and electron concentrations at different spatial locations. Such a study would show to what extent the proposed conservation of the RDC is violated by the energy dispersion of LO phonons, the electron-electron interaction, and the inelastic acoustic scattering.

Upon entering the QN region, hot electrons rapidly lose their excess energy in an integral number of optical-phonon emissions. For electrons whose kinetic energy is higher than the satellite-valley band edge the LO-phonon scattering mean free path is about 50–100 Å.[12] At lower energies, when intervalley transitions are forbidden, simple estimates give an LO-phonon mean free path of about 500 Å. This means that over a distance $\lambda \lesssim 10^{-5}$ cm all possible optical phonons are emitted. Further acceleration of electrons by a weak electric field in the QN region can be neglected, because the total potential drop in that region is estimated (Sec. III) to be of order 1 mV. Therefore we can assert that in most of the QN region, whose thickness $L \lesssim 1 \ \mu$m, Eq. (5) is satisfied.

Let us introduce a "phase" Φ of the current energy distribution. It is convenient to first change the reference point of energy to the edge of the conduction band in the QN region. We shall designate energies counted this way by a caret, viz. $\hat{E}$, $\hat{E}_F$, etc. The applied voltage determines the value of the emitter Fermi level, $\hat{E}_F$, reduced modulo $\hbar \omega$ into the energy interval $(0, \hbar \omega)$. This quantity, in units of $\hbar \omega$, defines the "phase" Φ, see Fig. 1(b). It determines the energy of electrons in the QN region, which arrive there from the emitter Fermi level after having emitted all possible LO phonons. Mathematically, the phase Φ is defined by

$$\Phi = \frac{\hat{E}_F[\text{mod}(\hbar \omega)]}{\hbar \omega} \ , \tag{6}$$

i.e., Φ is the remainder of $\hat{E}_F / \hbar \omega$.

Figure 2 shows the energy dependence of $\partial J / \partial E$, calculated (as discussed below, Sec. III B) for three different applied voltages. It is convenient to plot $\partial J / \partial \hat{E}$ in units proportional to the total current J_{tot}, e.g., as is done in Fig. 2, in units of $[\partial J(E_F)/\partial E]_B$, which is the differential density of the tunneling current at the Fermi level. The dimensionless function

$$\frac{\partial J / \partial \hat{E}}{[\partial J(E_F)/\partial E]_B}$$

is truly periodic in the applied voltage because the trivial variation of $\partial J / \partial \hat{E}$ with J_{tot} is eliminated. Due to their
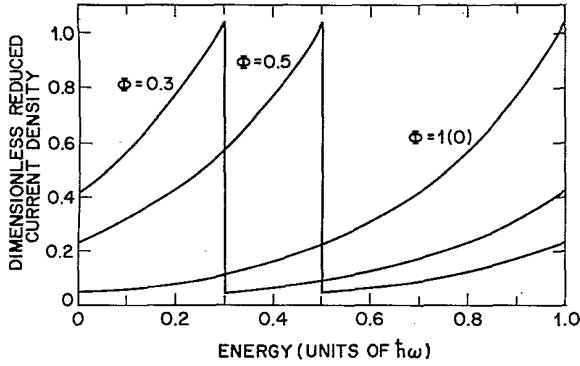
FIG. 2. Dependence of the dimensionless differential current density, $\partial J/\partial \hat{E}$ (in units of $[\partial J(E_F)/\partial E]_B$), on the energy $\hat{E}$ counted (in units of $\hbar\omega$) from the edge of the conduction band in the QN region. The three displayed curves, evaluated according to Eq. (20), correspond to applied voltages at which the phase Φ equals 0 (or 1), 0.3, and 0.5. Assumed parameters of the structure are as in Table I.

periodicity, the curves in Fig. 2, corresponding to three values of Φ, can be obtained from one another by a horizontal shift. The maximum of $\partial J/\partial \hat{E}$ occurs when $\hat{E}=(v+\Phi)\hbar\omega$. Electrons, originating from the Fermi level in the emitter, arrive at this energy. The value at the peak exceeds the initial value of $[\partial J(E_F)/\partial E]_B$ at the barrier interface approximately by 4%. This increase is due to the contributions from currents at $\hat{E}=\hat{E}_F-\hbar\omega$ and $\hat{E}=\hat{E}_F-2\hbar\omega$.

Note that the curves in Fig. 2 give a representation of the energy distribution of the current near the interface. As is evident, e.g., from the curve labeled 1(0), the distribution is by no means narrow on the scale of $\hbar\omega$. Therefore its representation by a δ function would not be a good approximation.

C. Dependence of the average mobility on the phase of the current energy distribution

Elastic scattering in the QN region is mainly owing to charged-impurity centers, whose concentration approximately equals twice the acceptor concentration. The differential current density in the QN region can be expressed in terms of the differential electron concentration $\partial n/\partial \hat{E}$ and the momentum relaxation time $\tau(\hat{E})$ as follows:

$$\frac{\partial J(\hat{E})}{\partial \hat{E}} = \frac{e^2 \tau(\hat{E})}{m}\frac{\partial n(\hat{E})}{\partial \hat{E}}F \ , \tag{7}$$

whence the total concentration n is given by

$$n = \int_0^{\hbar\omega}\frac{\partial n(\hat{E})}{\partial \hat{E}}d\hat{E} = \frac{m}{e^2 F}\int_0^{\hbar\omega}\frac{1}{\tau(\hat{E})}\frac{\partial J(\hat{E})}{\partial \hat{E}}d\hat{E} \ . \tag{8}$$

Defining the average mobility by the usual relation $J=en\mu F$, we have

$$\mu = \left[\frac{eJ_{\text{tot}}}{m}\right] \bigg/ \int_0^{\hbar\omega}\frac{1}{\tau(\hat{E})}\frac{\partial J(\hat{E})}{d\hat{E}}d\hat{E} \ . \tag{9}$$

Just like $\partial J/\partial \hat{E}$, the mobility μ in the QN region is a periodic function[13] of the phase Φ [provided that $\tau(\hat{E})$ does depend on energy]. Figure 3 shows the dependence $\mu(\Phi)$ for the cases when $\tau(\hat{E})$ is determined by charged-impurity and acoustic-phonon scattering mechanisms. The mobility behavior for these two mechanisms is "opposite" because $\tau(\hat{E})$ is an increasing function for impurity scattering and a decreasing function for acoustic phonons. We see that at $N_A \sim 10^{14}$ cm^{-3} and $T=4.2$ K the total mobility is determined mostly by the impurity scattering and is modulated by a factor of ≈ 3. The minimum in μ occurs when a large fraction of the current flows at low energies, where the impurity scattering is highest. Even at the minimum, the mobility is much larger than the equilibrium bulk mobility ($\mu_0 = \sim 6\times 10^4$ cm^2/V s) at the same impurity concentration and temperature. This mobility enhancement occurs because the average electron velocity in our ensemble is much higher than thermal.

D. Current formation in the quasineutral region

As far as the equilibrium band conductivity is concerned, the QN region is practically an insulator at liquid-helium temperatures.[10] Estimates (Sec. III) show that the nonequilibrium carrier concentration associated with the current in the "interesting" regime of the diode operation is of order 10^{12} cm^{-3}, which exceeds the equilibrium electron concentration in the QN region by several orders of magnitude. Consequently, the current in that region is space-charge limited (SCL).

The current-voltage characteristic of the QN region would, therefore, have the usual form of the Mott-Gurney law,[14] provided we could use the virtual-cathode approximation,[15−17] corresponding to a boundary condition of $F=0$. The variation of electrostatic potential $V(x)$ in the QN region under applied bias is illustrated in Fig. 1(a). Between the depleted region and the region of SCL current flow there is an inflection point in $V(x)$, because the net charge in these two regions is of opposite
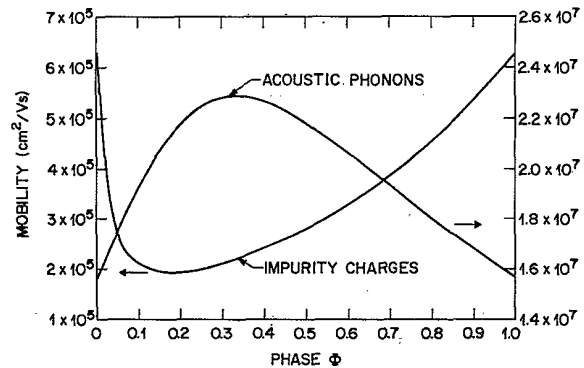

FIG. 3. Dependence of the mobility μ in the QN region on the phase Φ of the differential current density. The two curves correspond to mobilities calculated with the momentum relaxation due to charged-impurity and acoustic-phonon scattering mechanisms. Assumed parameters of the structure are as in Table I.

sign. There is no *a priori* reason why F should vanish in the vicinity of this point. A nonvanishing F would give a contribution to the voltage drop in the QN region—in addition to that obtained from the Mott-Gurney law. Nevertheless, we believe that the virtual-cathode approximation is valid here. This can be seen from the following argument.

Formation of the virtual cathode in a usual n^+-n^- junction is due to a large carrier concentration gradient that forces the diffusion current component to be larger than the total net current and requires an oppositely directed drift component to balance the books. In the present case, instead of the diffusion current, we have a large thermodiffusion current. To estimate the latter, we can use the Monte Carlo data[8] which indicate that, in the voltage regime of interest, the average electron energy at the end of the depletion layer is $\langle \hat{E} \rangle \gtrsim 0.1$ eV. In the QN region, this energy is dissipated in optical-phonon emission within a transition layer of order $\lambda \lesssim 10^{-5}$ cm. This gives the following estimate for the thermodiffusion current J_{TD} in the transition layer.

$$J_{TD} = \frac{S}{k} \mu n \frac{\partial T_e}{\partial x} \approx \frac{S}{k} \mu n \frac{\langle \hat{E} \rangle}{\lambda} , \qquad (10)$$

where S/e is the entropy transport parameter;[18] for nondegenerate semiconductors one has

$$\frac{S}{k} \approx \ln \left[\frac{(2mkT_e)^{3/2}}{4\pi^{3/2}\hbar^3 n} \right] \gtrsim 1 .$$

Since the effective driving force $\langle \hat{E} \rangle / \lambda \gtrsim 10^4$ eV/cm of thermodiffusion is much larger than that due to an estimated electric field ($\lesssim 100$ V/cm) in the QN region, the J_{TD} component is much larger than the net current. This results in the formation of a virtual cathode in the transition region.

III. EVALUATION OF THE CURRENT-VOLTAGE CHARACTERISTICS

The current-voltage characteristics of the diode can be calculated in a parametric form. It is convenient to take as a parameter the electric field F_B in the tunnel barrier. This field uniquely determines the tunneling current as well as its energy distribution near the barrier. The sequence of steps in the evaluation of the total voltage across the device is described below in detail.

A. Current density at the tunnel junction and its energy distribution

For the sake of simplicity, we assume that the aluminum fraction in the (AlGa)As barrier is constant, so that at flat bands the barrier is rectangular. Denote the barrier height by E_B (see Fig. 1). Estimates show that in the entire bias range of interest, $eV_B < E_B - E_F$, where $V_B = F_B d$ is the voltage drop in the barrier of thickness d. This means that the Fowler-Nordheim tunneling regime is never reached. At low temperatures, when the electron gas is degenerate, the tunneling current is given by

$$J_{\text{tot}} = A \int_0^{E_F} dE \int_0^E D(E_n) dE_n$$
$$= A \int_0^{E_F} D(E_n)(E_F - E_n) dE_n , \qquad (11)$$

where

$$A = \frac{em}{2\pi^2 \hbar^3} \qquad (12)$$

is the effective Richardson constant and $D(E_n)$ is the tunneling probability dependent on the transverse (to the barrier) part E_n of the incident-electron kinetic energy, calculated in the WKB approximation:

$$D(E_n) = \exp \left[-\frac{2^{5/2} m^{1/2}}{3e\hbar F_B} \right.$$
$$\times [(E_B - E_n)^{3/2}$$
$$\left. -(E_B - E_n - edF_B)^{3/2}] \right] , \qquad (13)$$

where E is referenced to the conduction-band edge in the emitter. As seen from Eq. (11), the differential current $(\partial J / \partial E)_B$ at the interface is of the form

$$\left[\frac{\partial J(E)}{\partial E} \right]_B = A \int_0^E D(E_n) dE_n . \qquad (14)$$

Numerical evaluation of $(\partial J / \partial E)_B$ has shown that in the bias range of interest, this quantity is exponential over more than 2 orders of magnitude. This allows us to obtain an accurate close-form approximation of the current by expanding the logarithm of $(\partial J / \partial E)_B$ near $E = E_F$ and retaining linear terms only. This gives

$$\left[\frac{\partial J}{\partial E} \right]_B \approx \frac{\partial J(E_F)}{\partial E} e^{-\gamma(1 - E/E_F)}, \quad E \leq E_F , \qquad (15)$$

where

$$\gamma = E_F D(E_F) \bigg/ \int_0^{E_F} D(E_n) dE_n \qquad (16)$$

and the total current is given by

$$J_{\text{tot}} = E_F \frac{\partial J(E_F)}{\partial E} \frac{1 - e^{-\gamma}}{\gamma} . \qquad (17)$$

B. Current density in the quasineutral region

As discussed above, the differential current density in the QN region equals the RDC, Eq. (4). To evaluate the RDC, we use the approximate expression (15) for the energy distribution of the tunneling current. It should be noted that the reference point of E in Eq. (15) is the edge of the emitter conduction band, which is related to $\hat{E}$, referenced to the band edge in the QN layer, by

$$\hat{E} = E + edF_B + eV_D , \qquad (18)$$

where V_D denotes the voltage drop in the depletion layer. Expressing the RDC in terms of $\hat{E}$, we have

$$\frac{dJ(\hat{E})}{d\hat{E}} \equiv G(\hat{E}) = \left[\frac{dJ(E_F)}{d\hat{E}}\right]_B \sum_{v=-\infty}^{\hat{E}_F/\hbar\omega-\Phi} \exp\left[-\gamma\left[1-\frac{\hat{E}+v\hbar\omega-edF_B-eV_D}{E_F}\right]\right] . \tag{19}$$

We have extended the lower limit of summation in Eq. (19) to $-\infty$, because contributions to the tunneling current from electrons at energies near the bottom of the Fermi sea are negligible compared to that from electrons at the Fermi level. The result of summation is

$$\frac{dJ(\hat{E})}{d\hat{E}} = \begin{cases} \left[\dfrac{dJ(E_F)}{d\hat{E}}\right]_B \dfrac{\exp[\gamma(\hat{E}-\hbar\omega\Phi)/E_F]}{1-\exp(-\gamma\hbar\omega/E_F)} & \text{for } 0\le\hat{E}\le\hbar\omega\Phi \\[4mm] \left[\dfrac{dJ(E_F)}{d\hat{E}}\right]_B \dfrac{\exp[\gamma(\hat{E}-\hbar\omega\Phi+\hbar\omega)/E_F]}{1-\exp(-\gamma\hbar\omega/E_F)} & \text{for } \hbar\omega\Phi\le\hat{E}\le\hbar\omega . \end{cases}$$

$$\text{(20a)}$$

$$\text{(20b)}$$

The differential current density, evaluated according to Eq. (20), has been plotted in Fig. 2.

C. Current-Voltage Characteristics: Numerical Example

In the numerical calculations, we have used the parameters listed in Table I. Based on these parameters, the elastic scattering is dominated by interaction with charged-impurity centers. The total concentration N_1 of charged scattering centers equals twice the acceptor concentration, $N_I \approx 2N_A$. Since the free-electron concentration in the QN is much less than N_I, we use the Conwell-Weisskopf approximation[19] for the momentum relaxation time:

$$\frac{1}{\tau(\hat{E})} = \frac{N_I\pi e^4}{2\epsilon^2 m^{1/2}\hat{E}^{3/2}}\ln[1+(\epsilon\hat{E}/e^2 N_I^{1/3})^2] . \tag{21}$$

Equation (21), substituted in Eq. (9), gives the dependence $\mu(\Phi)$ shown in Fig. 3. This dependence of the mobility on the phase Φ gives rise to an oscillatory variation of the voltage drop V_{QN} in the QN layer—calculated in accordance with the Mott-Gurney law,

$$V_{QN} = \left[\frac{32\pi J_{tot}L^3}{9\epsilon\mu}\right]^{1/2} . \tag{22}$$

The current-voltage characteristic is determined in a parametric form $J_{tot}(F_B)$, $V(F_B)$. It is evaluated in the following sequence: (a) For a given barrier field F_B, the current is determined by Eq. (11); (b) the voltage drop in the depleted layer and length W of the latter are given by their form in the depletion approximation:

$$V_D = \frac{\epsilon F_B^2}{8\pi e(N_D-N_A)} , \tag{23}$$

$$W = \frac{\epsilon F_B}{4\pi e(N_D-N_A)} ; \tag{24}$$

(c) with the obtained values of V_D and $V_B \equiv dF_B$, we determine $\hat{E}_F = E_F + eV_D + eV_B$ and then the phase Φ from Eq. (6); (d) with the calculated Φ, the mobility μ is determined by (9), using Eqs. (20); (e) with both J_{tot} and μ known, the voltage drop in the QN region is given by (22); (f) the total applied voltage is given by

TABLE I. Parameters used in the numerical calculations.

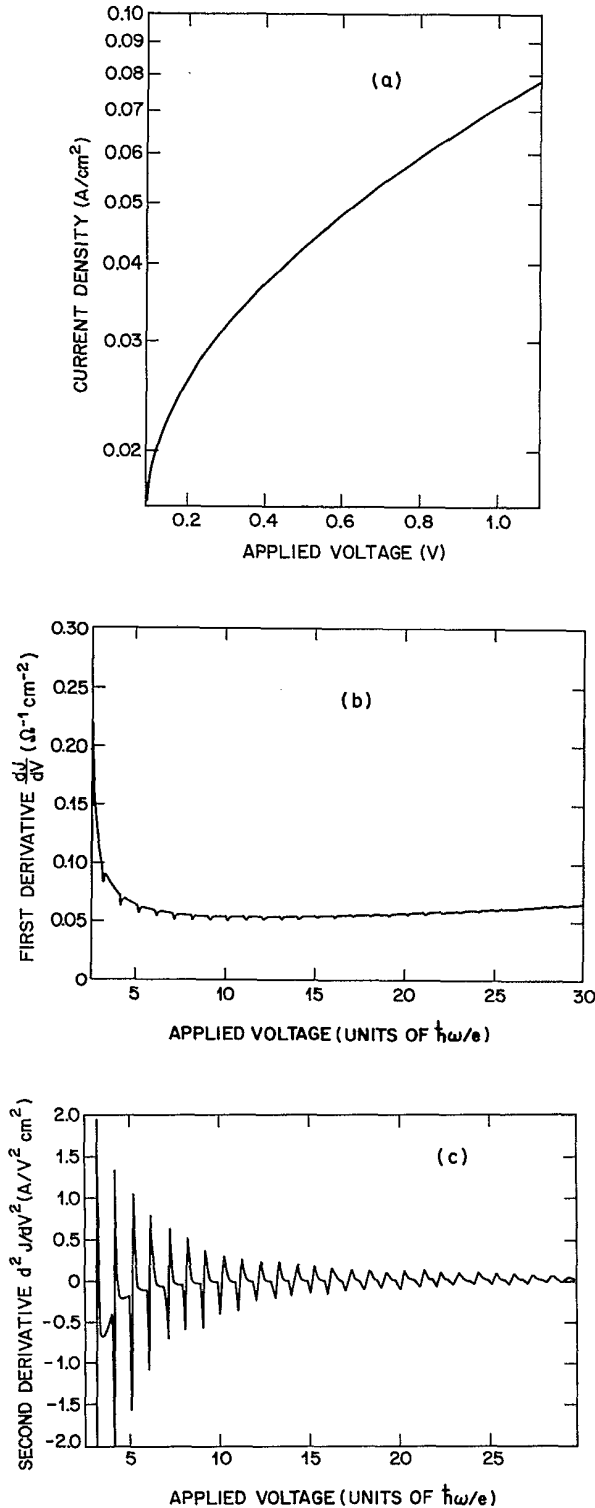| Assumed parameters	
Electron effective mass in GaAs (m)	$0.067m_0$
Electron effective mass in (Al,Ga)As (m)	$0.09m_0$
Optical-phonon energy $(\hbar\omega)$	36 meV
Barrier height (E_B)	0.2 eV
Barrier thickness (d)	170 Å
Electron concentration in the emitter	2×10^{18} cm^{-3}
Donor concentration in n^- layer (N_D)	2×10^{15} cm^{-3}
Acceptor concentration in n^- layer (N_A)	$0.1N_D$
Thickness of the n^- layer $(L+W)$	1 μm
Dielectric constant (ϵ)	12.9
Temperature (T)	4.2 K
Effective Richardson constant (A)	1.1×10^{10} A/cm^2 eV^2
Calculated parameters	
Fermi energy in the emitter (E_F)	87 meV
Fermi energy in the QN layer (E_F^{QN})	-4.9 meV
Equilibrium mobility in the QN layer (μ_0)	5×10^4 cm^2/V s
Equilibrium electron concentration in QN region (n_0)	10^9 cm^{-3}

$$V=(E_F-E_F^{ON})/e+V_B+V_D+V_{QN} \ , \qquad (25)$$

where E_F^{QN} is the equilibrium Fermi level in the QN region, referenced to its conduction-band edge.

Parameters assumed in Table I are similar to the experimental situation described in Refs. 2 and 3. In making a comparison with the experiment, we must first point out a discrepancy concerning the IV characteristics—apart from the issue of the current oscillations. Tunneling current, evaluated by the standard formula (11), turns out to be more than an order of magnitude lower than that reported in Refs. 2 and 3. The origin of this discrepancy is not understood. It cannot be explained by an incorrectly chosen barrier height, because the experimental characteristics are also steeper than the calculated ones. Although the absolute magnitude of the current is not crucial for our model of the current oscillations; it is important in comparative estimates, especially comparing the injected and the equilibrium conductivities of the QN region. Because of that, we have chosen to use an artificially large effective Richardson constant $A=80 \ \mathrm{A\,cm^{-2}\,K^{-2}}$, which is 10 times the value following from Eq. (12). This makes the current density close to the experimental values.[2]

The calculated IV characteristics and their derivatives are displayed in Fig. 4. We note that in the first-derivative plot [Fig. 4(b)], the oscillations manifest themselves as dips; this corresponds in the IV characteristics to bends lowering the current from its mean course. This behavior is in agreement with the experiment. Physically, in our model the current is depressed when more electrons in the QN region have lower energy—suffering higher scattering rate on impurities.

The relative amplitude of the current oscillations $\Delta J /J_{\mathrm{tot}}$ is of the order 10^{-3}, experimentally, and this is in excellent agreement with our estimates. Figure 5 shows the calculated voltage drop V_{QN} in the QN region as a function of the total applied voltage V. Consider the relative oscillations at $V=0.3$ V, where the voltage oscillation amplitude $\Delta V_{QN}\approx0.3$ mV. In this range, the current $J_{\mathrm{tot}}\approx0.03$ A/cm^2 [Fig. 4(a)] and $(\partial J_{\mathrm{tot}}/\partial V)_{V=0.3 \ V}\approx0.06 \ \Omega^{-1}\mathrm{cm}^{-2}$ [Fig. 4(b)]. Whence

FIG. 4. Current-voltage characteristics calculated with the parameters listed in Table I. (a) Current density J_{tot} vs the applied voltage. (b) First derivative $\partial J_{\mathrm{tot}}/\partial V$. To illustrate the periodicity, the applied voltage V is expressed in units of $\hbar\omega/e$. (c) Second derivative $\partial^2 J_{\mathrm{tot}}/\partial V^2$ vs the applied voltage in units of $\hbar\omega/e$. The oscillation amplitude decreases both because the quasineutral region shrinks with V and because the increasing current leads to a lower resistivity of the QN region. At higher voltages, approximately corresponding to the depletion of the entire n^- GaAs layer, the oscillations disappear.
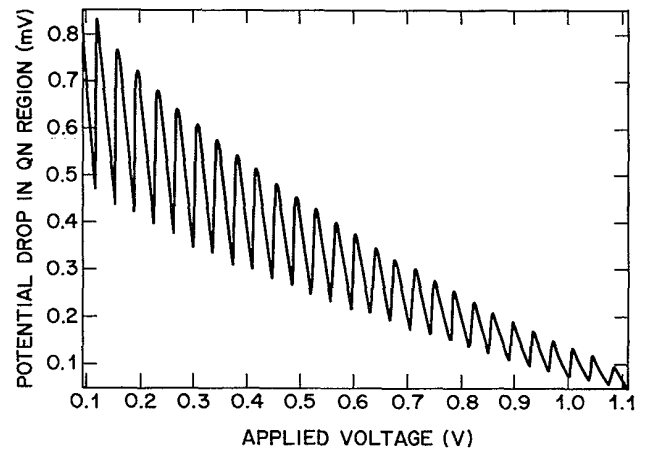

FIG. 5. Oscillatory voltage drop in the QN region as a function of the applied voltage.

we can estimate $\Delta J / J_{\text{tot}} = (\partial J_{\text{tot}} / \partial V) \Delta V_{\text{QN}} \approx 0.6 \times 10^{-3}$.

The calculated resistance of the space-charge-limited current in the range of $V = 0.3$ V corresponds to a resistivity $\rho \equiv V_{\text{QN}} / J_{\text{tot}} L \approx 200$ Ω cm. This is lower than the resistivity associated with the hopping conduction quoted in Refs. 2 and 3, which gives us ground to believe that hopping conductivity does not play an important role.

IV. CONCLUSION

The Hickmott experiment has attracted a considerable theoretical attention. Its importance lies in the fact that the observed current oscillations reveal certain peculiarities of the electronic transport in strong fields and over short distances—a situation common to modern semiconductor devices. The commonly known peculiar features of such transport are the velocity overshoot and the ballistic effects. The characteristic distances of those effects are determined by the fast processes of energy and momentum relaxation, respectively. In the present work, the experimentally observed current oscillations have been related to the conservation of another quantity, the reduced current density, which persists over much longer distances, determined by the relatively slow process of inelastic scattering by acoustic phonons. We believe, therefore, that this transport characteristic may prove useful for a wide variety of problems.

[1] T. W. Hickmott, P. M. Solomon, F. F. Fang, F. Stern, R. Fischer, and H. Morkoç, Phys. Rev. Lett. **52**, 2053 (1984).

[2] L. Eaves, P. S. S. Guimaraes, B. R. Snell, D. C. Taylor, and K. E. Singer, Phys. Rev. Lett. **53**, 262 (1985).

[3] L. Eaves, P. S. S. Guimaraes, F. W. Sheard, B. R. Snell, D. C. Taylor, G. A. Toombs, and K. E. Singer, J. Phys. C **18**, L885 (1985).

[4] J. P. Leburton, Phys. Rev. B **31**, 4080 (1985); Physica B+C **134B**, 32 (1985).

[5] J. R. Barker, Physica B+C **134B**, 2285 (1985).

[6] E. S. Hellman, J. S. Harris, C. Hanna, and R. B. Laughlin, Physica B+C **134B**, 41 (1985); E. S. Hellman and J. S. Harris, Phys. Rev. B **33**, 8284 (1986).

[7] J. Ihm, Phys. Rev. Lett. **55**, 999 (1985); see also comment by C. Hanna and R. B. Laughlin, *ibid.* **56**, 2547 (1986) and Ihm's reply, *ibid.* **56**, 2548 (1986).

[8] T. Wang, J. P. Leburton, K. Hess, and D. Bailey, Phys. Rev. B **33**, 2906 (1986).

[9] L. Eaves, F. Sheard, and G. A. Toombs, in *Physics of Quantum Electronic Devices*, Vol. 27 of *Springer Series in Electronics and Photonics*, edited by F. Capasso (Springer-Verlag, Berlin, 1990), Chap. 4.

[10] At any realistic compensation level the equilibrium concentration of band electrons in the QN region is negligible and has no effect on the conductivity of that QN region. At $T = 4.2$ K and $N_D \approx 10^{15}$ cm^{-3}, the equilibrium electron concentration in the QN region equals $\approx 3 \times 10^{11}$ cm^{-3}, while at a reasonable 10% level of compensation by acceptors, the electron concentration drops to 5×10^8 cm^{-3}.

[11] It would be rather meaningless to base such estimates on a requirement of strict electrical neutrality of the QN region, because the extent of that region is of the order of the Debye screening length. Electrical neutrality is a necessary requirement only in samples whose minimal linear dimensions much exceed the Debye length. In the experimental situation,[1,2] for $T = 4.2$ K, this condition is fulfilled at the level of the donor concentration, $N_D \approx 10^{15}$ cm^{-3}, and acceptor concentration $N_A \approx 10^{14}$ cm^{-3} (assuming 10% compensation). However, it fails at the level of band electron concentration $n \approx 10^{12}$ cm^{-3} in the QN region, which corresponds to a screening length $L_D = (\epsilon k T / 4 \pi n e^2)^{1/2} \approx 0.5$ μm.

[12] H. Shichijo and K. Hess, Phys. Rev. B **23**, 4197 (1981).

[13] The function $\mu(\Phi)$ is continuous as well as periodic. At a finite temperature, the function $\mu(\Phi)$ is also analytic. The apparent cusps at integral values of Φ (Fig. 3) are associated with the sharp edge of the Fermi function at E_F, reflected in the apparently discontinuous behavior of the RDC in Fig. 2.

[14] N. F. Mott and R. W. Gurney, *Electronic Processes in Ionic Crystals*, 2nd ed. (Oxford University Press, Oxford, 1948).

[15] W. Shockley and R. C. Prim, Phys. Rev. **90**, 753 (1953).

[16] A. A. Grinberg and S. Luryi, J. Appl. Phys. **61**, 1181 (1987).

[17] A. A. Grinberg, S. Luryi, M. R. Pinto, and N. L. Schryer, IEEE Trans. Electron. Devices **ED-36**, 1162 (1989).

[18] K. Seeger, in *Semiconductor Physics*, 2nd ed. (Springer-Verlag, Berlin, 1982), p. 81.

[19] E. M. Conwell, *High Field Transport in Semiconductors* (Academic, New York, 1967).